

Designing Watersheds for Integrated Development (DWID): Combining hydrological and economic modeling for optimizing land use change to meet water quality regulations

Ranjit Bawa ^{a,d,*}, Puneet Dwivedi ^a, Nahal Hoghooghi ^b, Latif Kalin ^c, Yu-Kai Huang ^a

^a Warnell School of Forestry and Natural Resources, University of Georgia, Athens, GA, 30602, USA

^b College of Engineering, University of Georgia, Athens, GA, 30602, USA

^c College of Forestry, Wildlife and Environment, Auburn University, Auburn, AL, 36849, USA

^d Department of Natural Resources and the Environment, University of New Hampshire, Durham, NH, 03824, USA



ARTICLE INFO

Keywords:

Land cover
Agriculture
Forestry
Landowners
Numeric nutrient criteria
Watershed management

ABSTRACT

By combining information on nutrient output from the Soil & Water Assessment Tool (SWAT) and secondary data on local profits from different crop types, we devise a profit maximization problem subject to dynamic water quality constraints, which become gradually more restrictive over time. The solution aims to detect the optimal allocation of land parcels by crop type that maximizes the total net present value of landowner profits throughout the watershed. Over a nine-year time span, our model construct is applied to the Little River Experimental Watershed (LREW) in South Georgia. Water quality constraints involve the landowner adhering to specific permissible limits on numeric nutrient criteria recorded at the watershed outlet under various scenarios, including i) NO₃-N constraints, ii) total phosphorus (P) constraints, and iii) concurrent NO₃-N and P constraints. In the most extreme case, a reduction in aggregate profits of \$24.1 million and \$8.1 million was observed for combined NO₃-N and P constraints relative to commensurate solo constraints on NO₃-N and P, respectively. The Designing Watersheds for Integrated Development (DWID) model could support policymaking for ascertaining trade-offs between economics and water quality channelized through direct and indirect land use change considering environmental regulations in Georgia and beyond.

1. Introduction

Long-term exposure to chemicals in the water supply are associated with a range of acute and long-term chronic illnesses [1,2]. Nitrate overconsumption, for example, can cause adverse effects on the health of children (e.g., neurodevelopment) and babies (e.g., methemoglobinemia or ‘baby blue syndrome’) [3]. Contaminated streams also harm the surrounding aquatic ecosystem life. For instance, excessive phosphorus concentrations cause increased occurrences of algal blooms, which deplete the water body of oxygen and can, in turn, potentially wreak havoc on freshwater animal communities [4].

However, unlike point sources such as sewage treatment plants and factories, the vagueness behind non-point source (NPS) water pollution makes it difficult to manage. It is the diffuse nature of contaminants – often originating from fertilizer application at the

* Corresponding author. Department of Natural Resources and the Environment, University of New Hampshire, 56 College Road, Durham, NH, 03824, USA.

E-mail address: ranjit.bawa@unh.edu (R. Bawa).

surface to eventual discharge into surface and ground waters – that result in contaminants being picked up by water flow over extensive areas of land.

NPS pollution itself results from both leaching to groundwater as well as land runoff to surface waters. Thus, the land use within a watershed can have a substantial effect on the water chemistry, commonly interpreted as quality indicators, of a river network. Forestlands, for example, are generally linked to better conditions in water quality health downstream [5–8]. Conversely, positive associations between certain land uses, namely modern industrial agriculture and degraded water quality, have also been well documented [9–12]. Identifying individual land parcels linked to elevated pollution levels downstream, however, remains challenging. Indeed, two interrelated themes that consistently emerge in the environmental and natural resources management literature are land allocation and water quality.

Research concerning land allocation and water quality must also be examined in the context of specific numeric nutrient criteria guidelines. The National Primary Drinking Water Standards (NPDWS), which apply to public water systems, set the Maximum Contaminant Level (MCL) for $\text{NO}_3\text{-N}$ at 10 mg/L. For rivers and streams, the EPA's recommended total Nitrogen criteria range from 0.12 to 2.18 mg/L and from 0.01 to 0.08 mg/L for total P across each of the nation's distinct 14 eco-regions [70]. While no explicit MCL associated with P currently exists, the EPA recommends total phosphorus concentration (as phosphorus) not exceeding 0.10 mg/L in streams not discharging directly into reservoirs and not exceeding 0.05 mg/L in streams discharging directly into reservoirs [13]. Such low concentrations make P monitoring particularly challenging. In addition to MCL's, Section 303(d) of the Clean Water Act requires states to submit a list of all waters that are not supporting their designated uses and need to have a Total Maximum Daily Load (TMDL) developed.

Although environmental laws designed to protect water resources largely exclude regular ongoing farming, silvicultural, and ranching activities, several federal and state policies still apply to farmers and forest landowners. Activities associated with converting timberland to agricultural crop production, for example, are not exempt from environmental regulations. In Georgia, water quality standards are based in part on numeric nutrient criteria. Nutrient criteria are established using eco-regions (Level III and IV), which provide a spatial basis for criteria development [14]. The Georgia Environmental Protection Division (GEPD) administers periodic water quality monitoring as part of the agency's efforts to manage NPSs for water pollution. Recent TMDL annual nutrient loads for respective total nitrogen and total phosphorus amounts in our study area, the Little River Experimental Watershed (LREW) in South Georgia, have been reported at 42,419 kg/year and 5778 kg/year, respectively [14].¹ In the event water quality problems become attributed to specific landowners, and the landowner fails to take remedial measures, incidents are referred to the GEPD for enforcement.

Future policies must draft potential water quality regulations consistent with the USEPA's method for deriving ambient water quality criteria for the protection of human health. The USEPA peer-reviewed technical guidance for developing additional numeric nutrient criteria for rivers and streams suggests the use of predictive relationships by applying empirical and mechanistic models [15]. Here, we apply an empirical economic model to a small watershed in South Georgia. We examine the interaction among competing environmental and financial pursuits on land use allocation and how they are likely to change over time. Our work contributes to water resource management literature in at least two aspects. First, we hope our relatively straightforward approach may provide indications to policymakers on where certain measures can be more effective in reducing non-point sources of nutrient runoff at the watershed outlet. Second, by ascertaining the prospect of likely land cover patterns across our considered watershed, we draw on conclusions reached in this study to better identify trade-offs in the context of future watershed quality programs. Although our analysis centers around the landowner and their combined profits, we note the practical infeasibility stemming from the landowner's (understandable) lack of clarity in interpreting water quality improvements downstream (i.e., watershed outlet), and thus perhaps their inability to implement suggested alternative crops on their land. Rather, our approach would seem to give more indications to policymakers as opposed to landowners.

Before elaborating on our approach further, it is necessary to consider the context of the methods we have used. Previous research in LREW has examined the application of the SWAT model with different periods and approaches [16–19]. Yet, the relationship between water quality and land cover is intricate and requires monitoring of water bodies and land management. Best management practices (BMPs), for instance, have been proven to reduce nutrient loadings from agricultural areas. In the case of filtration systems or vegetated systems (i.e., biofilters), the goal is to capture a portion of received runoff and in the process, channel it into the soil. The pollutants in that portion are thereby effectively prevented from penetrating the local river network. With advances in computing power, evolutionary computation and mathematical programming techniques such as genetic algorithms (GAs) have been increasingly used in determining the optimal placement of BMPs to attain water quality targets at watershed scales [20–22]. In another study, Shoemaker et al. [23] employed mixed-integer linear programming alongside evolutionary computations (i.e., scatter search and genetic algorithms) to jointly determine the optimal location, type, and cost of stormwater BMPs needed to meet water quality goals in urban watersheds. Genetic algorithms, however, can be time-intensive in comparison to classical optimization solvers and require a rather intricate grasp of elaborate parameters (e.g., crossover, mutation rate, fitness function). Limbrunner et al. [24] demonstrate a linear programming algorithm analog to a nonlinear optimization model that efficiently reproduced much of the same solution structure when optimizing the watershed scale placement of BMPs.

Classical optimization techniques typically take the form of minimizing costs subject to certain pollutant load criteria [22,25,26], or in the alternative, maximizing water quality under cost constraints [21,24,27,28]. Multi-objective optimization, whereby the

¹ Little River - Ashburn Branch, W. of Sycamore to Warrior Creek, situated in the Suwannee River Basin, Georgia, U.S.A.

researcher simultaneously solves multiple objective functions [20,29], has also been utilized in managing water resource problems. Additionally, uncertainties linked to a specific parameter have been modeled using stochastic programming [27,28,30]. For example, Jia & Culver [28] developed a robust optimization model that sought to minimize pollutant load reductions given various levels of reliability with respect to water quality standards in a Virginia watershed. Likewise, Zhou et al. [30] considered a small hypothetical watershed for which costs associated with pollutant removal were minimized subject to chance constraints describing pollutant removal efficiency.

The focus of our study concerns a group of private landowners in a Georgia watershed who face the task of allocating land for a given set of crops over a multi-period planning horizon. The influences of a range of hypothetical government policies limiting specific water quality parameters on land use decisions by the landowner and its subsequent impact on land cover evolution are considered. We seek to maximize aggregate landowner net profit, subject to prescribed limits on water quality indicators downstream. Selected scenarios allow gradual reductions in permissible nutrient concentration recorded at the watershed outlet. Three distinct watershed mandates are considered: 1) tightened restrictions in permissible $\text{NO}_3\text{-N}$ concentration 2) tightened restrictions in permissible P concentration, and 3) tightened restrictions in both $\text{NO}_3\text{-N}$ and P concentration. Trade-offs between environmental and economic interests are evaluated through measures of marginal changes in aggregate landowner net profit because of having to meet increasingly higher water quality criteria. By attaining a better understanding of landowner behavior through the perceived trade-offs between profit and environment, we hope to contribute to the design of prospective environmental programs to promote improved water quality. While prior work has also investigated programs of land allocation which rely on SWAT and optimization procedures (see Ref. [31]), our study is of relevance because of the increasing need for studies that offer guidance on-farm practices or configurations to decrease the environmental deterioration of water bodies.

We first describe the study area. The methodological framework follows, outlining the assumptions and inputs that feed our modeling technique. Highlighted results are presented for the linear programming problem under various scenarios defining different water quality mandates. The manuscript concludes with a discussion of the findings with an emphasis on policy recommendations and potential avenues for future research.

2. Characteristics of watershed

This study was conducted on the 334 km² LREW, located in the headwaters area of the Suwannee River in the Coastal Plain Physiographic Province basin near Tifton, GA (Fig. 1). The watershed overlays three counties (Turner, Tift, and Worth) in the state. Broad valleys supporting wide stream networks are typical of the local geography. The elevation of the watershed generally increases from south to north, with the highest elevations occurring in the northwest corner. Underlain by the Coastal Plain aquifer, the LREW

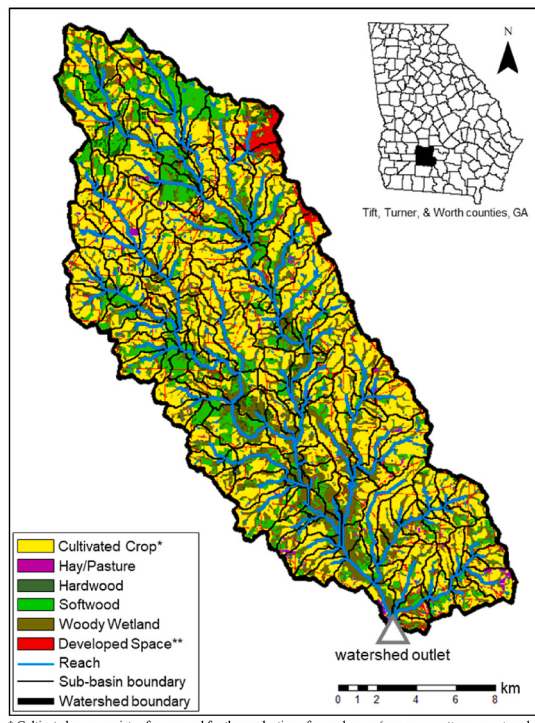


Fig. 1. Study area, the Little River Experimental Watershed, located in South Georgia, United States. Distribution of land cover across the watershed is illustrated using classification from the 2004 National Land Cover Database (NLCD).

consists primarily of low-gradient streams surrounded by higher gradient streams. Most of the soil classifies as a Tifton loamy sand, followed by Alapaha loamy sand with a high infiltration rate [32].

Streamflow and water quality of the LREW have been monitored by the United States Department of Agriculture Agricultural Research Service (USDA-ARS) since 1967; no permitted point source discharges exist in the watershed [18]. Climate is categorized as humid subtropical with a long growing season [33]; average annual precipitation and temperature are 1208 mm and 19.1 °C, respectively. Streamflow is likely attributable to 30% of annual rainfall, mainly composed of return flow from the local shallow aquifer, and to a lesser extent, direct surface runoff [34].

Although the LREW is agricultural-dominated, forests still occupy the landscape in a significant manner. Watershed land characteristics based on the 2004 National Land Cover Database (NLCD) is approximately defined as 51% row crops (primarily peanut, corn, and cotton), 16% evergreen forest, 2% deciduous forest, and 1% hay. Other notable categories include woody wetland (22%), which largely occurs on the borders of the stream network, and urban space (6%), mostly confined to a small northeast corner of the watershed.

3. Methodology

3.1. Synopsis

The SWAT model is initially calibrated and validated over a nine-year time frame, 1997 to 2005, to simulate NO₃-N loadings, P loadings, and surface runoff, at the watershed outlet. Calibrating for crop-related parameters which control plant growth produced average crop yields at the HRU level. In the end, annual data on crop profits, nutrient loadings, and surface runoff feed a dynamic linear optimization program that maximizes landowner profits subject to specific water quality constraints. Fig. 2 provides for a concise flowchart illustrating the steps involved.

3.2. SWAT model

3.2.1. Overview

The SWAT model is a process-based and semi-distributed, continuous time-step model that can simulate hydrology, crop growth, nutrients, and sediment loads [35]. SWAT is one of the most broadly applied large-scale watershed simulation models in Total Maximum Daily Load (TMDL) analyses and water resource planning. Its applications have included predicting the impact of land management practices on nutrient yields from agricultural land use in large complex watersheds with varying soils, land use, and management conditions over long periods [36,37].

We used ArcSWAT 2012 interface to set up the model using the 30 m Digital Elevation Model (DEM), Soil Survey Spatial Tabular (SSURGO 2.2) soils data, National Land Cover Dataset (NLCD), and National Agricultural Statistics Services (NASS) land use data. Precipitation, temperature, relative humidity, solar radiation, and wind data were obtained from Global Weather Data for SWAT (<https://globalweather.tamu.edu/>) (Table 1). We followed Liew et al. [19] and chose the Hargreaves method [38] for estimating potential evapotranspiration (PET). Using topographic information, the SWAT model divided the watershed into 198 sub-basins. Subsequently, each subbasin was divided into Hydrologic Response Units (HRUs) with unique combinations of land use, soil, and slope [39]. Three slope classes were used for HRU classification: 0–5%, 5–10%, and above 10%. The threshold of 20, 10, and 5% for soil, land use, and the slope was applied to reduce the number of HRUs (total 1272 across 198 sub-basins). We obtained an estimate of management operations (planting dates, fertilizer application rate and type, crops yield, and harvesting dates) for the LREW from the University of Georgia Cooperative Extension specialist (Dr. Dewey Lee, personal communication and <https://www.caes.uga.edu/extension-outreach.html>) and USDA-NASS (1997) (https://www.nass.usda.gov/Publications/National_Crop_Progress/). A three-year peanut-corn-cotton rotation was applied in the model for all the peanut, corn, and cotton fields. Amounts of 134 and 65 kg N/ha in the form of elemental nitrogen fertilizer were applied in corn and cotton fields, respectively. The amount of 50 kg P/ha of phosphorus fertilizer (as P₂O₅) was applied in both corn and cotton fields. For hay land use, urea (200 kg/ha) with two applications in May and June, and elemental P (60 kg/ha) were applied. We used ‘harvest only’ operation in SWAT that occurred twice a year. A baseflow separation technique [40] was used to initialize the value of the baseflow recession constant (ALPHA_BF). We made relative adjustments of ALPHA_BF during the model calibration.

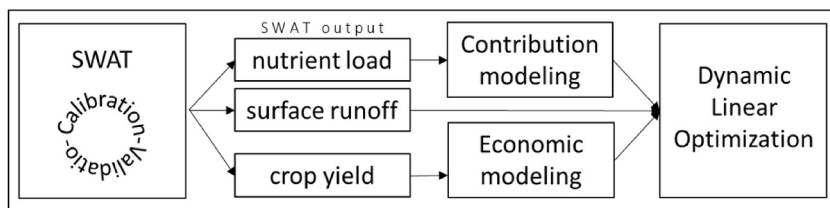


Fig. 2. Flowchart of the methodological process describing our study. SWAT outputs are combined with results from contribution modeling and crop profits before feeding a dynamic linear optimization problem. The term contribution modeling refers to the relative nutrient contribution of each sub-basin at the watershed outlet for each year and for each land cover type.

Table 1

Data feed used to produce SWAT simulations and subsequent dynamic linear programming problem. Listed data sources pertain to all years in our study period, 1997 to 2005.

	Parameter	Source
SWAT inputs	Elevation (30 m)	Digital Elevation Model (DEM)
	Soil series	Soil Survey Geographic database (SSURGO V2)
	Land cover type	National Agricultural Statistics Service (NASS)
	Precipitation	Precipitation Regression on Independent Slopes Model (PRISM)
	Temperature	Precipitation Regression on Independent Slopes Model (PRISM)
LP inputs	Nutrient loadings	SWAT output
	Surface runoff	SWAT output
	Crop yields	SWAT output
	Prices	National Agricultural Statistics Service (NASS)
	Costs	University of Georgia Cooperative Extension, Historical crop budgets

3.2.2. Calibration & validation

The Sequential Uncertainty Fitting algorithm (SUFI- version 2) in the SWAT Calibration and Uncertainty Programs platform [41, 42] was used to calibrate and validate the model for streamflow, nutrients (nitrate-nitrogen and total phosphorus), and sediment at daily time step at the outlet of LREW. The SUFI-2 combines optimization with uncertainty analysis. Uncertainties in the parameters result in model output uncertainties, quantified as the 95% prediction uncertainty (95PPU) band between the 2.5 and 97.5% levels of the cumulative distribution of an output variable using Latin hypercube sampling [42].

The observed data from the USDA-ARS gauging station at the main watershed outlet (<ftp://www.tiftonars.org/database>) between 1997 and 2005 were used with a four-year model initialization (1993–1996) followed by a five-year calibration (1997–2001) and two years model validation (2002–2003). To evaluate the model performance, we used two quantitative error statistics: Kling-Gupta efficiency (KGE) [43] and the Percent Bias (PBIAS). The KGE contains three components: correlation (r), the ratio between the mean of the simulated values and the mean of the observed ones (μ_s/μ_o), and variability ratio (σ_s/σ_o) between the simulated (s) and observed (o) variable; μ and σ are the mean and standard deviation of the variable, respectively:

$$KGE = 1 - \sqrt{\left\{ (r - 1)^2 + \left(\frac{\mu_s}{\mu_o} - 1 \right)^2 + \left(\frac{\sigma_s}{\sigma_o} - 1 \right)^2 \right\}} \quad (1)$$

KGE ranges from $-\infty$ to 1, with a value closer to 1 representing a relatively accurate model. KGE overcomes the disadvantage of Nash-Sutcliffe efficiency [44] in underestimating peak flow prediction [43]. PBIAS measures the average tendency of the predicted data to be larger or smaller than observed values. It also measures over- and underestimation of bias [45]:

$$PBIAS = \frac{\sum_{i=1}^n (o_i - s)}{\sum_{i=1}^n o_i} \times 100 \quad (2)$$

The optimum value for PBIAS is 0%, where values close to zero indicate better model prediction and overestimation is signified by PBIAS $< 0\%$, and underestimation indicates when PBIAS $> 0\%$ [46].

Calibration and validation of the model were conducted as one at a time calibration. In addition to parameters, we incorporate biophysical parameters for major crops in the LREW in our calibration process. Parameters controlling nutrients and sediment loads were indicated through a literature review [42,49]. Parameters controlling streamflow and plant growth were calibrated first, followed by sediment and phosphorus, and then nitrate-nitrogen parameters.

We used average annual USDA-NASS crop yield observed data (except for forest classes). After the streamflow was calibrated, crop parameters were adjusted to simulate crop yields (refer to Table S1 in SI). Average modeled yields for each crop were subsequently compared across the LREW with published yields for Tift county, retrieved from the University of Georgia [56].

3.3. Nutrient load assignment

3.3.1. Contribution modeling

To account for N and P loss and transformations at each subbasin, we used an approach that assesses nutrient load contributions from each subbasin over simulation periods at the watershed outlet (see Refs. [50–52]). Therefore, after calibrating and validating the SWAT model, we defined a virtual rain gauge for each sub-basin in the watershed. The rain gauge was then switched off in successive series to find the contribution percentage of nutrient loads remaining at the watershed outlet from each sub-basin. The software R V.4.0.2 with extension package SWATplusR [53] was employed as a part of this analysis by interacting with our SWAT project to help execute efficient simulation runs across all sub-basins (for both $\text{NO}_3\text{-N}$ and P).

SWAT computes contribution percentages, using a routing scheme, based on the channel network that connects the outlets of sub-basins to the watershed's primary outlet. The exact nutrient loading to be routed for a given sub-basin, i , was estimated accordingly. We refer to this estimated amount as an adjusted nutrient loading per sub-basin, written as:

$$B_i = b_i * a_i \quad \forall i = 1, 2, \dots, 198 \quad (3)$$

where B , adjusted nutrient loading, was calculated as the product of original nutrient loading amount, b , and nutrient loading contribution percentage, a .

3.3.2. Land use assumptions

Adjusted nutrient loadings calculated at the sub-basin level were further broken down by land use. The model framework considers six land uses: Bermuda hay, corn, cotton, peanut, and forest, classified as softwood and hardwood. The default SWAT setup was used for forest management, which assumes no fertilization, no thinning, and a maturity of 10 and 30 years for deciduous and evergreen forests, respectively. An additional land use category, extra, which is meant to capture barren land, is also included. Crop type in our analysis is therefore composed of a total of seven classes.

Nutrient loadings for each crop in each subbasin were calculated as the weighted average of loadings, weighted by SWAT reported crop yields at the HRU level. As an initial step, daily NO₃-N and P loadings, corresponding to each HRU by crop type for each year were obtained from calibrated SWAT output. Values were summed over days to arrive at annual values corresponding to each HRU. Computing the average across all years and HRU for each crop then served as the basis for constructing relative weights among crop type. The created crop coefficients were subsequently multiplied by the adjusted nutrient load recorded at each sub-basin i to derive specific nutrient allocation by crop type. Land classified as Extra was assumed to produce zero nutrient loadings. An analogous procedure applies to the surface runoff calculations, also projected at the crop level.

3.4. Economic modeling

Adopting present value (PV) considerations, landowner profit was discounted back to the initial period. Using the notation below, π and Π reflect respective average annual profits and PV of average annual profits:

$$\pi_t = p_t y_t - w_t \forall t = 0, 1, 2, \dots, 8 \quad (4)$$

$$\Pi_t = \pi_t / (1 + r)^t \quad (5)$$

where p is the annual crop price assessed in \$/kg, y is annual crop yield (produced from SWAT output) measured in kg/ha, and w is annual crop cost reported in \$/ha. The time is denoted by t where 0 is synonymous with the year 1997. The discount rate is captured by r , set at an interest rate of 4.1%.² Similar to nutrient loading assignments, zero profits were assumed for land designated as Extra. A depiction of relative comparisons in profit amounts by the crop is presented in Fig. 3.

Annual price data for agricultural crops were acquired through USDA NASS [54]. Prices for forest crops, softwood and hardwood, were calculated using historical stumpage values sourced from TimberMart-South [55]. Average annual costs were estimated by referencing historically expected cost budgets for non-irrigated land in the study area [56]. Hardwood and softwood forest costs were calculated as the sum of average annual costs consisting of fertilizer and herbicide application, machine planting, mechanical site preparation, and prescribed burning [57]. Cost budgets as described were assumed constant across years.

In eq. (5), replacing π with c , meant to capture estimated conversion costs associated with switching from one land use class to another, yields an analogous left-hand-side (LHS) value, C_t , or the PV of incurred conversion costs for a particular year. These necessary conversion costs are considered when our analysis is extended to the profit maximization problem (described in the following section). In this way, land moving between aggregate land use classes, agriculture, and forestland, becomes dependent on relative returns. A major component in land preparation from forest to agriculture is clearing the land of stumps. Based on consultation with field experts (academia and industry), it was estimated that excavator services required to pull and pile stumps post clear cut would charge at a minimum, the equivalent PV of \$4942/ha for pine and \$6177/ha in the case of hardwoods.

Costs associated with having to convert Bermuda to another crop potentially were also derived. Estimates were based on incurred costs for prepping the land with necessary fertilizer and herbicide application. Our average watershed corn yield of 7841 kg/ha would require approximately 134 kg N/ha, suggesting a cost of \$168.03/ha. In addition, the herbicide glyphosate is effective at killing green weeds. Assuming a common recommended application of 3.36 kg/ha of herbicide, further costs were calculated at \$3.30/kg or \$11.09/ha. Hence, conversion costs from the Bermuda crop were set equal to the PV of a total future outflow value, \$179.12/ha.

3.5. Dynamic linear optimization

Table 1 presents a comprehensive list of the inputs feeding the dynamic optimization model (as well as input parameters for the preceding SWAT runs). **Table 2** provides short descriptions of the primary notation used in our optimization model. Our profit maximization problem spans the following dimensions, old crop type, new crop type, sub-basin, and year (captured in respective j , J , i , and t subscripts). The dynamic optimization framework seeks to maximize aggregate landowner profit subject to constraints on land use and downstream water quality. The sum of individual landowner net profit is interpreted as a measure of social welfare in the LRW. We presume that because changes to consumer surplus would be minimized if crops were traded in the market, total economic surplus becomes a function of producer surplus and thus may be roughly captured through a representation of producer surplus (i.e., aggregate

² The discount rate as applied here was calculated based on the average federal funds rate during the time-period 1997 to 2005, plus a spread of 50 basis points.

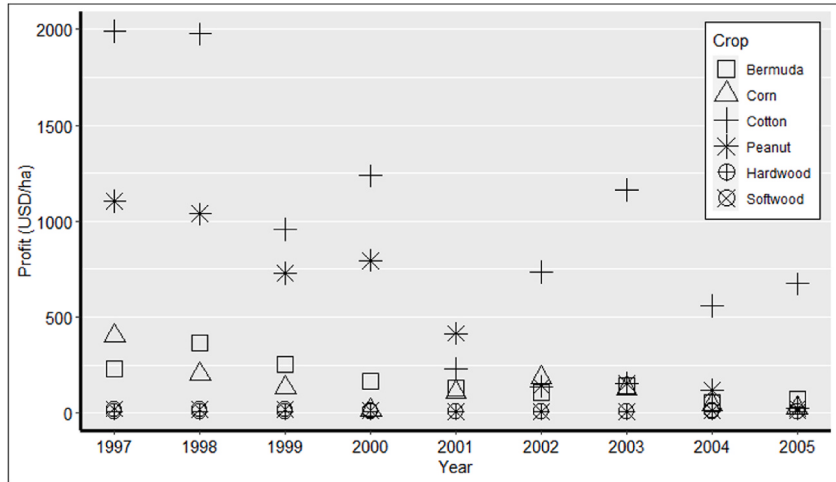


Fig. 3. Crop profits (US \$/ha/year) in the study area. Profits are discounted back to the initial period (1997) using an interest rate of 4.1%.

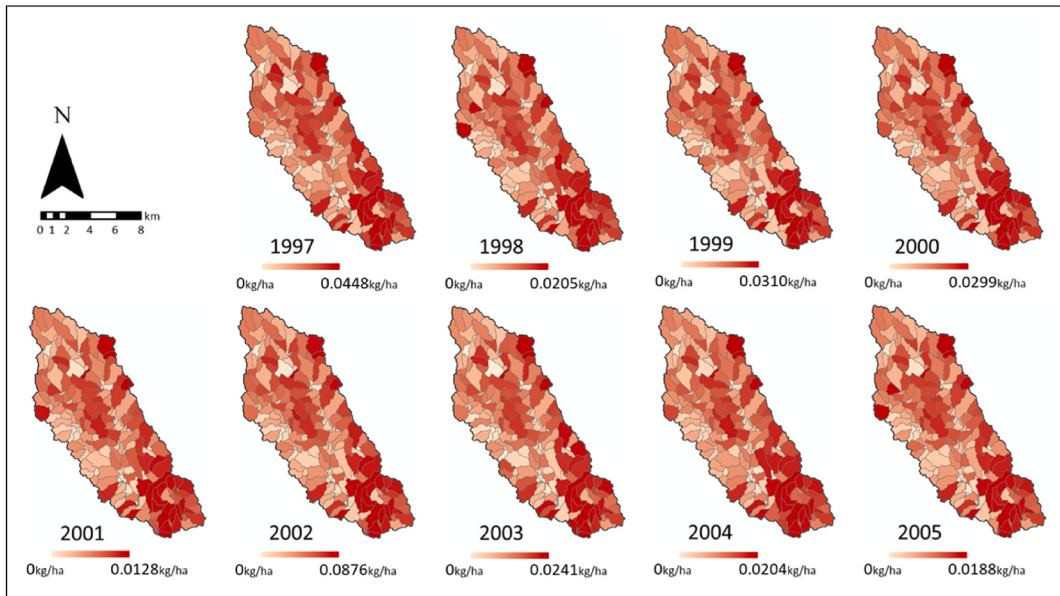


Fig. 4. Spatial distribution of NO₃-N load contribution from each subbasin to the watershed outlet for different time-steps.

watershed profit). The model was solved in MS Excel with What'sBest V.16.0 [58] solver to find an efficient solution to the optimization problem.

The objective function solves for the annual land allocation (L) for each of 198 sub-basins that result in maximum net profit (Z) across the watershed over the nine years, 1997 to 2005.³ Mathematically, the profit maximization problem with land area (A) constraints is expressed as follows:

$$\text{Max } Z = \sum_j \sum_i \sum_t (\Pi_{j,i,t} X_{j,i,t}) - \sum_j \sum_i \sum_t \sum_J (C_{j,i,t,J} X'_{j,i,t,J}) \quad (6)$$

subject to land use restrictions:

³ Using sub-basins as the unit for land use configuration in this manner, as opposed to finer scales such as hydrological response units (HRUs), may result in improved optimizing efficiency by decreasing the search space of spatial optimization [59].

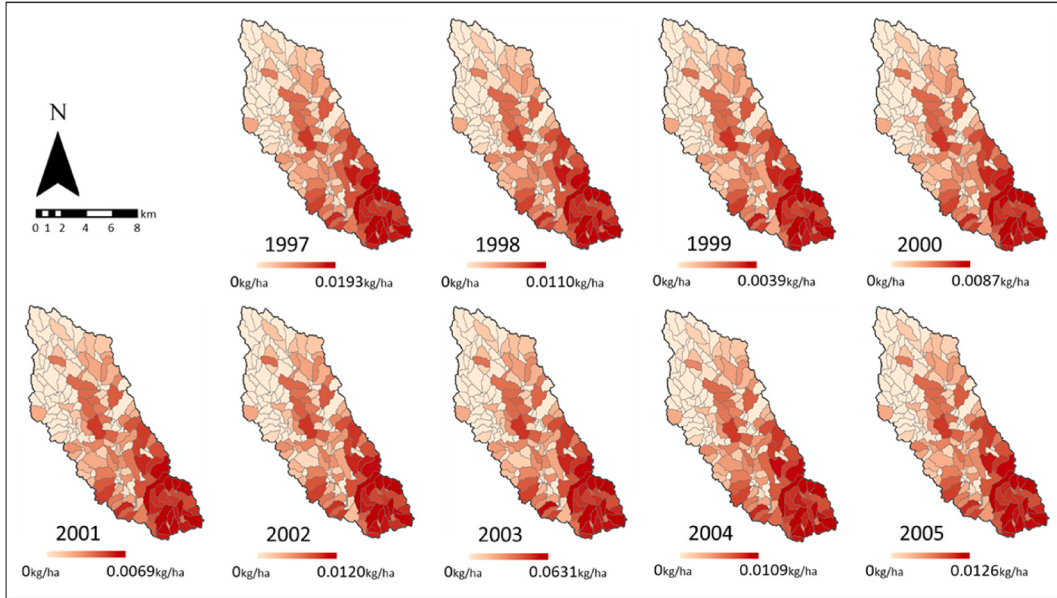


Fig. 5. Spatial distribution of P load contribution from each subbasin to the watershed outlet for different time-steps.

Table 2
Description of notation used in Optimization model.

Notation	Definition	
Z	max. net profit	[variable]
L	land allocation	[variable]
X	hectares harvested	[decision variable]
X'	hectares converted	[decision variable]
Π	profit	[parameter]
C	costs	[parameter]
A	land area	[parameter]
S	surface runoff	[parameter]
B	nutrient loading	[parameter]
D	nutrient limit	[parameter]
i	space (sub-basins)	[index]
t	time step (years)	[index]
j	old land use (crops)	[index]
J	new land use (crops)	[index]

$$\sum_j X'_{j,i,t,J} \leq X_{j,i,t} \forall j, i, t \quad (7)$$

$$X_{j,i,t} \leq L_{j,i,t} \forall j, i, t \quad (8)$$

$$\sum_j L_{j,i,t} = A_{i,t} \forall i, t \quad (9)$$

$$\sum_j L_{j,i,t} = \sum_j X_{j,i,t-1} + \sum_{J=j} \sum_j X'_{j,i,t-1,J} - \sum_{j=J} \sum_{J \neq j} X'_{j,i,t-1,J} \forall i, t, J \neq Extra \quad (10)$$

where X and X' are decision variables referring to hectares harvested and hectares converted, respectively. At each time step and sub-basin, the sum of converted hectares to all crops from each crop must not exceed crop hectares harvested (7). The second constraint, eq. (8), ensures the annual harvested crop area was less than or equal to allocated land for a given particular sub-basin. Continuing from this, eq. (9) confirms the sum among allocated crop area for each sub-basin and year is equal to the physical area of each subbasin (and trivially) at each period.

Our model works to project the hypothetical evolution of land cover across the LREW through several years, the basis of which is the initial year of land allocation. Land classed as Extra was set constant to initial year land composition in 1997. For remaining crops, eq. (10) shows how the land allocation was deduced as a function of the decision variable, optimal hectares harvested (X'); that is, for a

given sub-basin, allocated annual cropland was set equal to the allocated annual cropland in the previous year plus the sum of annual converted hectares from all old crops to each new crop minus total annual converted hectares to all new crops from each old crop.

The water quality constraint sets the level of restriction on nutrient concentration for each year in the study period:

$$\sum_j \sum_i (B_{j,i,t} / S_{j,i,t}) X_{j,i,t} \leq D_t^\gamma \forall t \quad (11)$$

where the LHS in the above captures the measured nutrient concentration in the watershed each year. Here, the notation B follows from eq. (3) and S stands for surface runoff. Load, originally measured in kg/ha, was converted to mg/ha. Likewise, surface flows were converted from mm to L. Transforming units in this manner produce units in mg/L, consistent with the theoretical nutrient limit denoted by D . The superscript γ references nutrient type, i.e., NO₃-N or P.

In the initial year, our water quality limit was set equal to the total annual concentration as derived on the right-hand-side (RHS) of (11). In subsequent years, D_t follows a linear percentage reduction from the preceding year:

$$D_t^\gamma = \sum_j \sum_i (B_{j,i,t} / S_{j,i,t}) X_{j,i,t} \quad \text{for } t=0 \quad (12a)$$

$$D_t^\gamma \leq D_{t-1}^\gamma (1 - q) \quad \text{for } t \neq 0 \quad (12b)$$

where q is the nutrient percent limit reduction, although the formal policy may be unlikely to consist of successive reductions to set concentration limits per succeeding year, the conjecture allows a useful perspective in visualizing the impact of increasing water quality restrictions on changes in land cover. The ending limits applied in respective models for NO₃-N and P were based on the maximum percentage reduction permitted before the solver renders the solution infeasible. More precisely, prescribed nutrient limit percentage declines were construed by simply a) determining the smallest percentage reduction that first triggers a marginal change in maximized aggregate profit; b) determining the smallest percentage reduction that first triggers the optimization model infeasible; and c) composing a series of six equally spaced intervals between the two percentages as defined in preceding steps a) and b).

Thus, the imposed limit in our model is primarily a function of the computed aggregate nutrient concentration. The application of our model in a different setting (i.e., watershed) would derive limits directly dependent on the total size in the area, nutrient loadings, and surface flows considered.

Our analysis begins with a Base scenario where no reductions to the maximum concentration limit are implemented. Relative to this scenario, our optimization problem assumes annual percentage declines in the concentration limit for subsequent years. We consider gradual tightening of NO₃-N limits, P limits, as well as concurrent NO₃-N and P constraints. We identify the minimum feasible limit on the right-hand-side (RHS) of our water quality constraints for each case. Similarly, we make a note of the minimum percentage decline in our RHS water quality limit to trigger a profit decline relative to the Base scenario. In total, 21 scenarios, as well as a Base scenario, are evaluated. The scenarios presented in Table 3 can be interpreted as hypothetical restrictions (from our Base scenario) mandating a percentage reduction in nutrient concentration as measured at the watershed outlet. Included are seven changes in NO₃-N limit: 48% (N1), 52% (N2), 56% (N3), 60% (N4), 64% (N5), 68% (N6) 72% (N7); seven changes in P limit: 14.75% (P1), 15.25% (P2), 15.75% (P3), 16.25% (P4), 16.75% (P5), 17.25% (P6), 17.75% (P7); and seven simultaneous changes in respective NO₃-N and P limits: 48%, 14.75% (NP1), 49.16%, 15.08% (NP2), 50.33%, 15.42% (NP3), 51.50%, 15.75% (NP4), 52.66%, 16.08% (NP5), 53.82%, 16.42% (NP6), 54.99%, 16.75% (NP7). Therefore, N1 to N7 (as well as P1 to P7, and NP1 to NP7), refer to completely different scenarios, differentiated by the percentage reduction from base, each solved for the entire period of the model.

4. Results

4.1. SWAT calibration and validation

The calibration process for the LREW started with 36 hydrologic and biophysical parameters. After 1000 simulations, the most

Table 3

Created scenarios based on water quality limits corresponding to a gradual tightening in constraints. Twenty-two scenarios are devised in total including a common Base scenario (defined by limits for NO₃-N and P constraints that remain constant over time). Percentage declines for each of the three categories (NO₃-N, P, and NO₃-N & P) were devised based on equal intervals, starting with the percentage triggering an initial change in profits and ending with a percentage representing the maximum threshold permitted by the model.

NO ₃ -N	Percent decline	P	Percent decline	NO ₃ -N & P	Percent decline ^a
N1	48.00	P1	14.75	NP1	48.00, 14.75
N2	52.00	P2	15.25	NP2	49.16, 15.08
N3	56.00	P3	15.75	NP3	50.33, 15.42
N4	60.00	P4	16.25	NP4	51.50, 15.75
N5	64.00	P5	16.75	NP5	52.66, 16.08
N6	68.00	P6	17.25	NP6	53.82, 16.42
N7	72.00	P7	17.75	NP7	54.99, 16.75

^a Percent declines refer to constraints on NO₃-N and P respectively.

sensitive flow and biophysical parameters were identified and are listed in [Table 4](#) in order of decreasing sensitivity. The most sensitive parameters were effective hydraulic conductivity of the alluvium in the main channel (CH_K2.rte), groundwater delay time (GW_DELAY.gw), the fraction of growing season when leaf area begins to decline (DLAI.plant.dat), runoff curve number 2 (CN2.mgt), and available water capacity of the soil layer (SOL_AWC.sol). Parameter values should be considered after calibration to avoid unrealistic simulations. For instance, the fitted values for SOL_AWC in the SWAT model for crops and forest soil ranged from 0.06 to 0.07, which was comparable to the measured weighted average SOL_AWC of 0.057 for the Tifton soil series by Hubbard [\[60\]](#). CN2 for the main crops and forest (evergreen and deciduous) were reduced by 12% resulted in a better adjustment to streamflow predictions. The model fit was deemed satisfactory for streamflow calibration and validation with a daily KGE of 0.80 and 0.71 and PBIAS of -2.5 and 3.8, respectively ([Fig. S1](#)). The observed streamflow, the model best fit, and the 95 PPU band for calibration and validation periods are shown in [Fig. S2](#).

After the model was calibrated for hydrology and biophysical parameters, the narrow ranges for selected parameter values were fixed, and the model was calibrated for sediment load at the watershed outlet using 14 parameters. Following calibration of sediment load, total phosphorus (P) and nitrate-nitrogen ($\text{NO}_3\text{-N}$) loads were calibrated ([Table 5](#)).

The most sensitive parameters for sediment load were the exponent parameter for calculating sediment reentrained in channel sediment routing (SPEXP.bsn), a linear parameter for calculating the maximum amount of sediment that can be reentrained during channel sediment routing (SPCON.bsn), and the cover factor for the effect of land cover on erosion (USLE_C.plant). The SPEXP and SPCON are parameters used to calculate the maximum amount of sediment that can be transported from a reach. The fitted value for SPEXP and SPCON in our model was 1.210 and 0.001, respectively. The daily KGE was 0.43 and 0.57 for the calibration and validation period, respectively, with PBIAS of -2.5% for the calibration period and 0.2% for the validation periods ([Table 5](#)).

The most sensitive P parameters were residue decomposition coefficient (RSDCO.bsn), phosphorus enrichment ratio for loading with sediment (ERORGP.hru), and the cover factor for the effect of land cover on erosion (USLE_C.plant) ([Table 4](#)). The fitted value for RSDCO and ERORGP was 0.07 and 2.58, respectively. The daily KGE for P load was 0.63, with PBIAS of 0.4% for the calibration period and KGE of 0.35 with PBIAS of 2.8% for the validation period. The model performance for daily P at the watershed outlet evaluated as "satisfactory" with daily KGE >0.35 and PBIAS $\leq \pm 30\%$. The lower KGE for the validation period was expected because the observation data for P loads were sparse for that period (compared with daily observations for streamflow).

The most sensitive N parameter was denitrification threshold water content (SDNCO.bsn) ([Table 4](#)). The daily KGE for $\text{NO}_3\text{-N}$ load was 0.50 with PBIAS of -7.9% for the calibration period and the KGE of 0.46 with PBIAS of -19% for the validation period. The model performance for daily $\text{NO}_3\text{-N}$ load at the watershed outlet was considered "satisfactory" with daily KGE >0.35 and PBIAS $\leq \pm 30\%$.

4.2. Nutrient contribution

Upon calibration and validation in SWAT, nutrient loadings linked to a given HRU for each day for each year were summed across days to arrive at annual values before averaging across all years for each HRU. A comparison of nutrient loadings by crop type is presented in [Fig. S3](#) using a log scale. Boxplots in panel 5a reveal the highest $\text{NO}_3\text{-N}$ loadings observed for Bermuda crop, averaging 0.622 kg/ha per year; the second highest was corn, averaging 0.014 kg/ha per year; followed by cotton, 0.001 kg/ha per year, and peanut, 0.00018 kg/ha per year. $\text{NO}_3\text{-N}$ loadings were even lower for forest, with hardwood averaging 0.00012 kg/ha per year and softwood associated with an average annual $\text{NO}_3\text{-N}$ load of virtually zero. Similarly, average annual P loadings in panel 5b were lowest for forest. Here, softwood was associated with slightly higher loads, estimated at 0.023 kg/ha per year, compared with 0.021 kg/ha per year for hardwoods. Bermuda again was reflective of the highest nutrient load out of the six crops at 0.396 kg/ha per year. Like Bermuda, cotton shows a fairly large number of outliers in the upper fence, averaging 0.252 kg/ha per year. Peanut and corn trail behind with estimated average annual loads of 0.081 and 0.072 kg/ha, respectively.

When we account for and subsequently incorporate a measure of nutrient decay based on the downstream travel time of a nutrient, loads were reduced significantly. While P loss mainly occurred through sedimentation, for $\text{NO}_3\text{-N}$ the primary process behind decay is denitrification. A graphical interpretation is offered in [Figs. 4 and 5](#), which show for all years how adjusted $\text{NO}_3\text{-N}$ and P loads compare across individual sub-basins, respectively. More precisely, the values mapped in both figures may be referred to as $B_{i,t}$ (continuing with notation from above), the adjusted nutrient load for each sub-basin at each time step. Amounts derived for sub-basins located in the southern part of the watershed generally correlated with higher loads. Because our model transforms calculated load amounts into concentration estimates before analysis, for added perspective, comparable amounts of surface runoff are presented for each sub-basin throughout the years in [Fig. 6](#). Compared to nutrient content, runoff amounts emerge as evenly distributed throughout the watershed for any given year.

4.3. Crop yield calibration

Calibrated versus observed values for all crop types are reported in [Fig. S4](#). For corn, cotton, and peanut, respective relative percentage differentials (from calibrated to observed) were 5.99%, 13.76%, and -8.13%; likewise calibrated yields for bermuda differed by -3.66% on average across the eight years, compared to observed values. Meanwhile, calibrated yields for both forest types were slightly higher compared to observed yields across the eight-year study period on average, for both hardwood and softwood at 2.84% and 1.39% respectively.

Table 4

The most sensitive streamflow, total suspended solids (TSS), total phosphorus (TP), and nitrate ($\text{NO}_3\text{-N}$) parameters and fitted, minimum, and maximum values used for calibration period using the Soil and Water Assessment Tool Calibration and uncertainty Program (SWAT-CUP).

Parameter	Description	Land use	Fitted value	Method ^a	Min. value	Max. value	p-value
Parameters sensitive to flow							
CH_K2.rte	Effective hydraulic conductivity of the alluvium in the main channel (mm/hr)		1.34	v	0	30	0
GW_DELAY_gw	Groundwater delay time (days)		33	v			0
CN2.mgt ^b	Runoff curve number 2	Row crops Forest (HW) Forest (SW) Cotton	68 73 48 0.8 0.006	r r r v r	-0.2 -0.02 -0.02 0.15 -0.2	0.2 0.02 0.02 1 0.4	0.002 0.002 0.002 0.004 0.023
DLAI.plant	Fraction of growing season when leaf area begins to decline						
SOL_AWC.sol	Available water capacity of the soil layer (mm $\text{H}_2\text{O}/\text{mm}$ soil)						
Parameters sensitive to sediment load							
SPCON.bsn	Maximum amount of sediment that can be reentrained during channel sediment routing		0.001	v	0.0001	0.01	0
SPEXP.bsn	Exponent parameter for calculating sediment reentrained in channel sediment routing		1.2	v	1	1.5	0
USLE_C.plant	Cover factor for the effect of land cover on erosion	Cotton	0.34	v	0.001	0.5	0.016
Parameters sensitive to P load							
ERORGP.hru	Enrichment ratio for loading with sediment		2.58	v	0	5	0
RSDCO.bsn	Residue decomposition coefficient		0.07	v	0.02	0.1	0.017

^a v indicates the existing parameter value is to be replaced by a given value. r means an existing parameter value is multiplied by (1+ given value).

^b CN values are final absolute fitted values in the model.

Table 5

The simulated Kling-Gupta efficiency (KGE) and the Percent Bias (PBIAS) for nitrate ($\text{NO}_3\text{-N}$) and TP loads (kg/ha), sediment, and streamflow during calibration and validation periods at the watershed outlet.

Simulation period	NO ₃ -N		TP		Sediment		Streamflow	
	KGE	PBIAS	KGE	PBIAS	KGE	PBIAS	KGE	PBIAS
1997–2001 (calibration)	0.50	-7.9	0.63	0.4	0.43	-2.5	0.80	2.5
2002–2003 (validation)	0.46	-19.0	0.30	17.2	0.57	0.2	0.71 ^a	3.8 ^a

^a For streamflow, validation simulation period was 2002–2005.

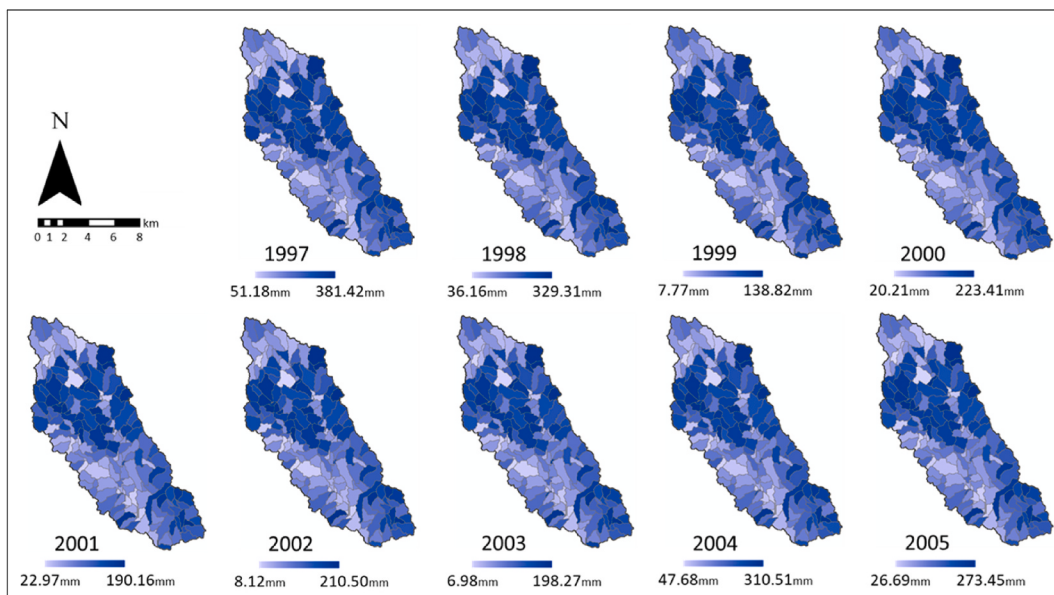


Fig. 6. Spatial distribution of surface runoff by subbasin at different time steps.

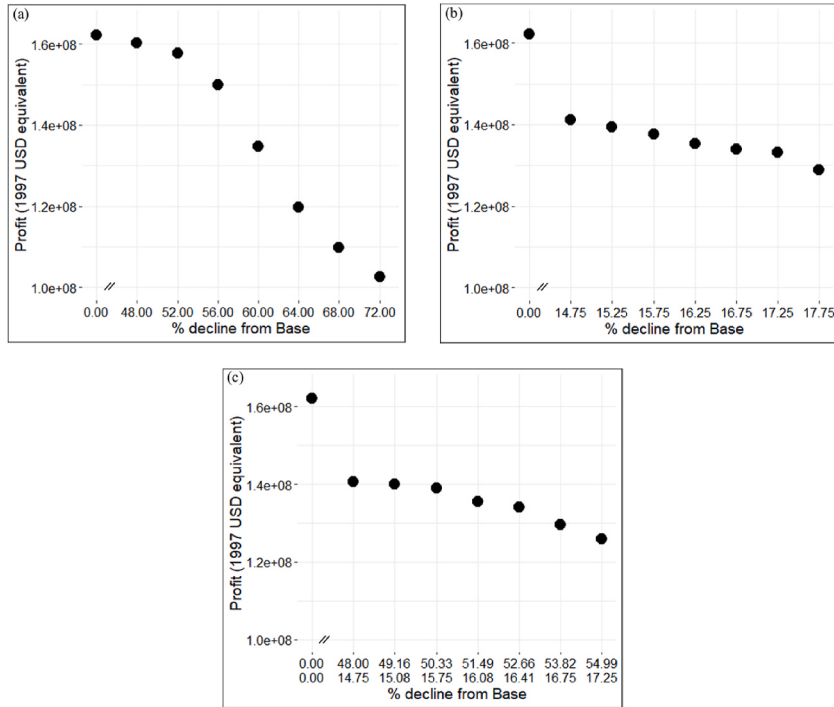


Fig. 7. Change in maximized welfare for linear percentage declines in the water quality constraint pertaining to NO₃-N limit (a), P limit (b), and both NO₃-N & P limits (c), from Base scenario over the study period. In Fig. 9(c), the first row of the x-axis refers to NO₃-N constraints and the second row shows constraints on P.

4.4. Optimization

We multiplied the LHS by a factor of a million in eq. (11) to produce nutrient concentration amounts in mg/L, as shown in Table 6. The initial year records comparatively high concentrations for both NO₃-N and P. Amounts reach a high of 0.0319 mg/L and a low of 0.0001 for NO₃-N; compared with a maximum 0.1029 P mg/L and minimum 0.0215 P mg/L.

Measures of aggregate landowner welfare for each of the scenarios listed in Table 3 are presented in Fig. 7. In the Base scenario, maximum aggregate profits for the watershed reach \$162.1 million; water quality limits on NO₃-N concentration and P concentration were estimated at 0.0319 mg/L and 0.1029 mg/L for all years, respectively. Examined in Fig. 7(a) are changes in welfare from tighter NO₃-N constraints, while P constraints are held constant at 1997 levels for all years. Not surprisingly, as yearly constraints defining the maximum concentration of NO₃-N become gradually more restrictive (or alternatively, as percentage reductions to the RHS gradually increase), aggregate profits decline. The waning profits appear to decrease at an increasing rate, given a linear percentage decline in water quality limits. Indeed, N1 (or the first decline of 48%) has a marginal effect on profit levels, dropping roughly 1.9 million from Base. In the most extreme scenario, N7, a 72% decline in the maximum allowable limit each successive year from 1997, yields \$102.6 million, equivalent to an approximate \$59.5 million in cumulative loss from Base. (b) illustrates the decline in profits from successively tighter P constraints holding NO₃-N constraints constant. Contrasted with Fig. 7(a), aside from the significantly greater plunge in profits occurring from Base to P1 (14.75%), the remaining downward trend in profits also takes general concave form, albeit on a different scale. Profit under the P1 scenario equates to \$1411 million, a nearly \$20.9 million drop from Base. When the percentage decline was increased to P7 (17.75%), aggregate watershed profit was reduced to \$128.8 million. Fig. 7(c) assumes concurrent changes in NO₃-N and P constraints relative to our Base scenario. Profit follows a similar path to the general shape presented in Fig. 7(b), characterized by a relatively large initial dip. For the combined case, profit reaches a low of \$125.8 million in the NP7 scenario.

To understand the exact land use transformations driving deteriorated profits, we refer to Fig. 10, which expose the majority land use class at the sub-basin level (based on cumulative acreage over the years) for all scenarios under prescribed changes to limit constraints for NO₃-N (Fig. 8(a)), P (Fig. 8(b)), and concurrent changes in NO₃-N and P (Fig. 8(c)). The common base scenario in the top left corner for all three panels shows the composition of land use across the LREW. In this case, the watershed was dominated by the cotton crop. In terms of the percentage of real acreage over the nine-year period, cotton composes almost 59% of all land, with combined hardwood and softwood areas occupying just over 4% of the watershed. The land class Extra accounts for ~23% of total lands in the watershed (and based on our modeling approach, remains constant in all scenarios). However, except for two relatively small sub-basins, the land use maps produced in Fig. 8 reflect the fact that Extra land fails to account for primary land cover under any of the remaining sub-basins. It becomes clear from Fig. 8(a) that softwood increasingly permeates the watershed, as land progressively converts from the highest profitable crop, i.e., cotton in the study area. In the N7 scenario, successive declines of 72% to the NO₃-N

Table 6

Annual nutrient concentration for the LREW at watershed outlet. Results presented in mg/L for the Base scenario.

Year	NO ₃ -N	P
1997	0.0319	0.1029
1998	0.0002	0.0684
1999	0.0009	0.0696
2000	0.0004	0.0572
2001	0.0001	0.0382
2002	0.0009	0.0387
2003	0.0004	0.0318
2004	0.0001	0.0251
2005	0.0001	0.0215

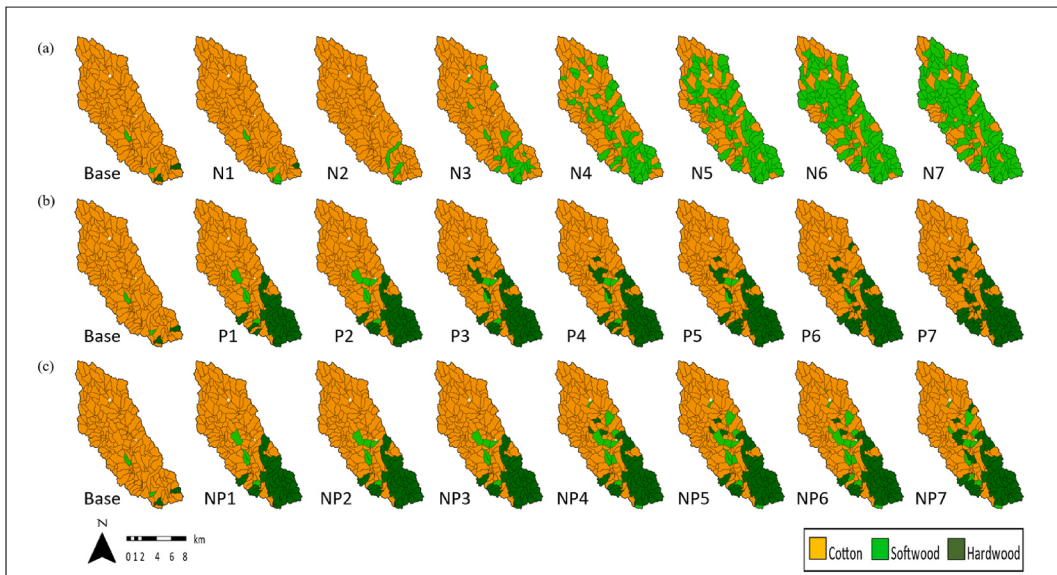


Fig. 8. Progression of land cover across the watershed for the different NO₃-N (a), P (b), and combined NO₃-N & P (c) scenarios considered. Percentages indicate a decline from the common Base scenario. Colors are representative of the dominant land use in each sub-basin. (For interpretation of the references to colour in this figure legend, the reader is referred to the Web version of this article.)

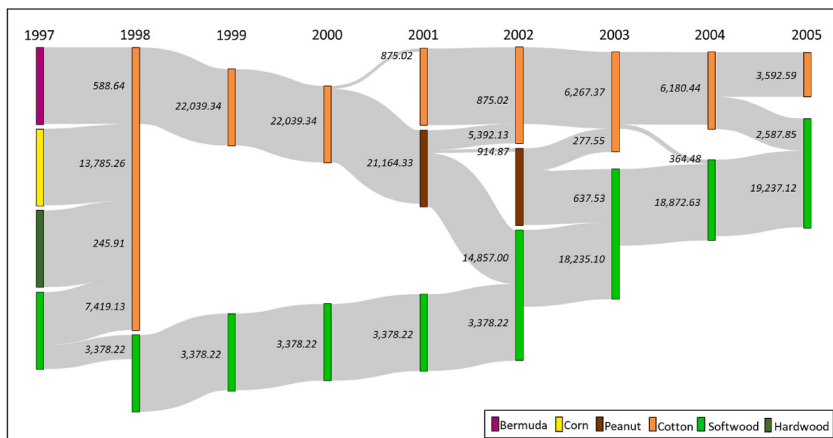


Fig. 9. Sankey diagram highlighting changes in land use class over time steps in the N7 scenario. The width in bands dictating land use flow is directly proportional to the relative contribution from old crop to new crop type; total number of hectares moving out of old crop and into new crop are denoted in italics.

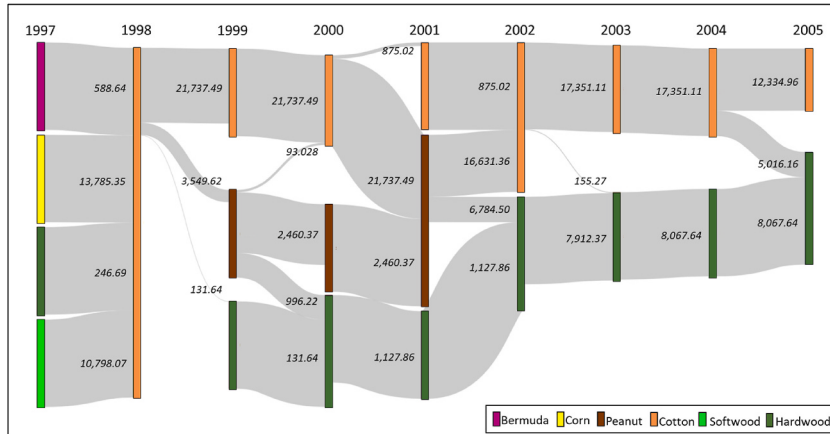


Fig. 10. Sankey diagram highlighting changes in land use class over time steps in the P7 scenario. The width in bands dictating land use flow is directly proportional to the relative contribution from old crop to new crop type; total number of hectares moving out of old crop and into new crop are denoted in italics.

water quality constraints expose softwood as the primary crop in most sub-basins throughout the watershed. In terms of percent of the actual area, this equates to nearly 35% of all land cover. The N7 scenario also shows the area of cotton slashed by nearly half from Base (to ~30%), while hardwood now makes up just less than a tenth of a percent of all lands contained in the watershed. When P constraints were made more restrictive, holding NO₃-N constraints constant, it was hardwood rather than softwood that came to infiltrate the watershed, primarily the bottom half. The initial tightening of constraints to P1 involves the few prior hardwood-dominated sub-basins multiplying and, to a lesser extent, softwood as well. Though, when constraints were tightened three percentage points further to P7, the few patches of hardwood-dominated sub-basins disappear. Under P7, the cotton remains the principal crop, composing 45% of the watershed, followed by hardwood which grows to over 13% of land cover. As in Fig. 8(b), Fig. 8(c) also depicts a strong forest presence in southern sub-basins after the initial change to NP1, which continues to steadily grow up until NP7. Unlike Fig. 8(b) however, a closer examination reveals relatively more softwood patches as well as a few sub-basins located further up north also converting to softwood.

Sankey diagrams shed additional perspective on land use progression in scenarios N7 (Fig. 9) and P7 (Fig. 10).⁴ Here, the flows between years represent a transition in land use from one year to the next, where width is directly proportional to the relative contribution from old crop to new crop type. For example, the band starting from Bermuda in the first column (in both (a) and (b)) designates the complete transition of land from Bermuda in 1997 to cotton in 1998. It should be noted that linear programming is well known to provide sparse solutions where only a few variables are selected (as seen in Figs. 9 and 10). Since the simplex algorithm searches for solutions on the vertices of the feasible region, following an optimal policy implies a reduction in heterogeneity among crop selection, which may in turn lead to possible deterrence in adoption by landowners.⁵

Dual values for binding constraints in our linear program, commonly termed shadow prices, are presented in Table 7 for select model runs. Values in this table reflect the decline in landowner profits given a unit decrease, defined as 0.000001, in the constant term (i.e., RHS) of a particular water quality constraint. We highlight the N7, P7, and NP7 scenarios, along with N1, P1, and NP1 scenarios for added context. The first two columns, referring to NO₃-N constraints, reveal dual prices tend to increase every year, the largest occurring in 2004 and 2001 under N1 and N7, respectively. For these years, we may state that tightening the constraint by one unit causes the objective value to decrease on a per unit basis of \$2111.49 under N1 and \$40,326.96 under N7. Comparatively, dual prices associated with P constraints under N1 and N7 were minimal. Under P1 and P7 scenarios, all dual prices associated with NO₃-N constraints were zero. Concerning P constraints, dual prices reach a max of \$769.02.96 and \$1915.85 for respective scenarios P1 and P7. The last two columns show respective dual prices for NP1 and NP7. As was the case in P1, in NP1, dual prices linked to constraint changes associated with NO₃-N were zero; prices linked to constraint changes associated with P, however, were higher when compared to N1 and P1 scenarios. Similarly, NP7 dual prices exceeded those in N7 and P7 scenarios for both NO₃-N and P constraints.

4.5. Sensitivity analysis

Running the optimization problem with simultaneous NO₃-N and P constraints can provide additional output to ascertain other individual effects from water quality mandates as well as any notable interacting effects. Under changes to both NO₃-N and P

⁴ A Sankey diagram for the NP7 scenario followed a similar pattern to illustrations for N7 and P7 but is not presented to conserve space.

⁵ A simple example may serve to illustrate the referenced reduction in crop heterogeneity. Consider for a moment that only two land use options (x, y) are permitted, for which three optimal solutions exist: $(0, 1)$, $(1, 0)$, and $(\frac{1}{2}, \frac{1}{2})$. In such a case, our model will always return a solution of $(0, 1)$ or $(1, 0)$.

Table 7

Dual prices (in 1997 US \$) associated with yearly constraints for NO₃-N and P are presented under selected scenarios. Six scenarios are presented below. These include the initial change from Base scenario and the most extreme case as it relates to: NO₃-N (N1 & N7) limits, P (P1 & P7) limits, and simultaneous NO₃-N and P (NP1 & NP7) limits.

	Year	N1	N7	P1	P7	NP1	NP7
NO ₃ -N	1998	135.42	944.81	0.00	0.00	0.00	1397.16
	1999	0.00	3344.46	0.00	0.00	0.00	0.00
	2000	0.00	11,838.81	0.00	0.00	0.00	6896.51
	2001	963.14	40,326.96	0.00	0.00	0.00	0.00
	2002	1852.18	0.00	0.00	0.00	0.00	34,059.02
	2003	1195.49	0.00	0.00	0.00	0.00	37,702.85
	2004	2111.49	0.00	0.00	0.00	0.00	77,486.36
	2005	0.00	0.00	0.00	0.00	0.00	172,407.15
P	1998	107.32	0.00	0.00	990.41	549.77	694.90
	1999	107.32	0.00	628.55	1207.09	0.00	834.71
	2000	107.32	0.00	691.52	1386.54	712.82	935.70
	2001	107.32	0.00	655.97	1514.33	682.15	950.94
	2002	107.32	0.00	769.02	1845.62	801.11	1142.27
	2003	70.98	0.00	581.47	1915.85	614.93	1051.32
	2004	0.00	0.00	298.98	1330.34	301.15	549.77
	2005	0.00	0.00	350.50	1621.37	353.67	660.39

constraints from Base, we observe the steady increase in hardwood and softwood tends to reflect hybrid traits of the individual NO₃-N and P scenarios previously considered. The progression of land use patterns may be analyzed more closely by examining certain combinations of specific scenarios. In each of the following three distinct sets, we note equal percent reductions defining the combined (NP) constraint and those identifying solo (N, P) constraints (as confirmed in Table 3).

- (i) N1, P1, and NP1
- (ii) N2, P4, and NP5
- (iii) N3, P5, and NP7

Under i) derived welfare estimates were virtually the same across all three scenarios; in ii), profits under NP5 were \$23.6 million less than what they were under N2 and \$1.2 million less than under P4; and in iii), profits are \$8.1 million less in NP7 than what they were under P5 and \$24.1 million less compared to N3. These findings show that the combined effect of requiring both water quality constraints to be met appears to exert greater losses in aggregate watershed welfare versus only having to consider lone NO₃-N or P constraints, as right-hand side limits tighten. This is expected and can be explained in part by the reduced feasible region of our optimization problem, a consequence of incorporating a second (concurrent) water quality constraint. However, it also observed that the scale of loss experienced in profits between solo constraint and combined constraint scenarios behave quite differently (as water quality limits tighten) according to specific nutrient content. For example, the \$1.3 million loss in profits between the P scenario (P4) and NP scenario (NP5) in set (ii) grows to a \$8.1 million loss in set (iii); comparatively, the \$22.1 million loss in profits between the N scenario and NP scenario in set (ii) gets slightly raised to \$24.1 million in set (iii).

Indeed, the biophysical and socioeconomic variation across a landscape undoubtedly complicates management decisions since every hectare of a given land class is not of equal value in generating a particular ecosystem service [61]. However, estimates as just described are notable in that they show, in monetary terms, the degree to how much crop cover can be maintained while maintaining compliance with water quality standards. Also provided is a sense of expected impact on welfare based on competing water-related policies. In our case, results indicate the possibility to reduce nutrient concentration considerably within a moderate range of total profit losses (~20% at the most). Such information can play an integral role in helping set amounts for potential ambient tax or subsidy schemes, commonly based on the water quality of the resource receiving the pollutant; assuming the appropriate zone for measuring concentrations in the water body has been identified [62].

The Sankey diagrams further examine the interflow between different land use types in the most extreme cases associated with changes to NO₃-N and P constraints, i.e., the N7 and P7 scenarios. Undoubtedly, these were the scenarios in which most land use changes took place as the model encouraged the transition from agriculture to the forest, due to tighter water quality constraints. Figs. 9 and 10 are meant to visually highlight the degree of land use transition over the study time frame. The number of land use transitions observed could increase or decrease dramatically, dependent upon reported crop profits and associated crop loadings. Yet, we note the likely practical feasibility from agriculture to forest remains questionable, and therefore, the significant crop conversion required to meet water quality constraints may manifest as a social planner's problem. Those areas that struggle to produce good yield (perhaps marginal lands) should be targeted first.

Our optimization problem takes the general form of maximizing a real function subject to certain resource (water quality) constraints. Accordingly, in the case of a less-than-or-equal constraint, such as a resource constraint, a dual price represents the value of having one more unit of the resource represented by that constraint; in our case, we measure the amount the objective deteriorates as the RHS of the constraint was decreased by one unit. As observed in Table 7, the highest price was observed for the NP7/2005 scenario related to the NO₃-N constraint. While even the highest observed dual price was low in terms of calculated welfare (less than one

percent), all else equal, overall sensitivity emerges as higher in $\text{NO}_3\text{-N}$ constraint linked dual prices and, in many instances, significantly higher. Such data can aid in making informed land planning decisions for meeting environmental standards. For example, it would be much costlier for the aggregate of landowners residing in the watershed to have to comply with a unit decrease in $\text{NO}_3\text{-N}$ concentration compared with P. At the minimum, a range of dual price estimates tied to various scenarios can provide landowners with better planning opportunities for reducing systematic risk while complying with various water quality criteria.

5. Discussion

Our discussion primarily concerns examining trade-offs involved in jointly managing land use decisions (i.e., profit) and water quality.⁶ In this context, Pfister et al. [64] seem to suggest the land/water trade-off rests more on the location of cultivation rather than characteristics of (agricultural) crop cover at a global level. Figs. 4 and 5 reveal that after accounting for nutrient decay, adjusted loads amounts were higher in sub-basins located in the southern part of the LREW, nearer the watershed outlet. This appears logical, given that sub-basins closer to the outlet would be characterized by lower associated travel time and hence, less nutrient decay. Because part of P gets carried with sediment and sediment deposits, it reasons that (in the case of P) two factors, reactions and deposition, may play a prominent role in explaining the spatial variation observed in nutrient loadings. Succeeding derivations of average annual concentration amounts per the watershed fell well within ranges reported in prior work [65,66]. Based on data between 1974 and 2003, Feyereisen et al. [66] derived mean annual nutrient concentrations between 0.14 and 0.23 $\text{NO}_3\text{-N}$ mg/L and 0.19 to 0.27 P mg/L for five sub-watersheds contained within the larger LREW. Likewise, for the two decades that overlap our study time frame, Bosch et al. [65] report average annual concentration amounts of 0.13 $\text{NO}_3\text{-N}$ mg/L and 0.10 P mg/L from 1990 to 1999 and 0.11 mg/L for both $\text{NO}_3\text{-N}$ and P from 2000 to 2009. Cho et al. [17] use the SWAT model to evaluate the water quality effects of conservation practice alternatives in the LREW and report validation results with wide ranging errors, from -25.7% for TN to -42% for P.

In our results, the higher concentrations in 1997 (for both $\text{NO}_3\text{-N}$ and P) were due to the large initial year allocation to traditional row crops (corn) within the watershed (Table 6). To compare with MCLs defined earlier, the 0.0319 mg/L $\text{NO}_3\text{-N}$ computed at the watershed outlet in 1997 is well within the maximum limit of 10 mg/L and remains negligible for the duration of the simulation period. On the other hand, the corresponding 0.1029 mg/L of P just breaks the EPA's recommended total phosphorus concentration of 0.10 mg/L in streams not discharging directly into reservoirs. This P reading was arguably somewhat unexpected since the LREW is not particularly known for water quality issues. After the first year, P concentrations persist slightly above naturally occurring background levels (~0.02 mg/L) but below an amount worthy of triggering (periodic) algal blooms.

It remains critical to visualize not only the overall changes in land cover that are likely to occur because of stricter water quality mandates but also the relative impacts associated with adhering to maximum allowable amounts set for one water quality parameter (i.e., $\text{NO}_3\text{-N}$) compared to another (i.e., P). It is clear from the results (Fig. 8) that under progressively tighter limits, the watershed gradually gets converted to forestlands before the model is rendered infeasible. Under changing $\text{NO}_3\text{-N}$ constraints, this manifests in the form of softwood making up primary land use in most sub-basins by N7 (Fig. 8(a)). In the case of firmer P constraints (Fig. 8(b)), hardwoods grow the most, eventually taking over softwoods as well, but to a lesser extent than the prior softwood domination observed in the end under $\text{NO}_3\text{-N}$ constraints. Also noted was the steep rise in hardwoods from Base to P1 versus Base to N1 scenarios. In both the individual N and P scenarios (Fig. 8(c)), the sub-basins that convert to majority forestland seem most prevalent along the southern reaches of the watershed. Such spatial patterns may be caused by affiliation with higher local nutrient content. If indeed the case, it seems plausible that these would be some of the first sub-basins to flip to land use more conducive to meeting lower concentration limits enforced at the watershed outlet.

Thus, for constraints on P, and especially $\text{NO}_3\text{-N}$, interventions aimed at improving water quality are likely to occur at the detriment of agriculturally productive land. These findings agree with a recent study investigating trade-offs between agricultural productivity and near-identical parameters describing water quality in a New Zealand catchment [67]. The authors suggest that agricultural land losses can be partly offset by an improvement in production on land less subject to nutrient loss. Although yield maximization, while reducing the pressures on land, can itself coincide with lower water-use efficiencies [64].

Understanding how water quality impacts of proposed land use changes compared to impacts of baseline land use regimes is equally important. In this context, baseline land use may be defined as 1998 allocations since the initial land composition in 1997 was assumed fixed. In the Base case scenario, annual $\text{NO}_3\text{-N}$ concentration amounts derived for the LREW increased ~61% from 1998 to 2005; P concentration rose about 29% during the same interval. The observed growth in concentration amounts is not necessarily surprising, even though water quality limits get more restrictive each year. One may interpret that under the Base scenario, defined water quality limits are too large to influence land allocation decisions. Thus, in the Base scenario, landowners continue to produce the most profitable crop in any given year. Percentage declines in $\text{NO}_3\text{-N}$ concentration from 1998 to 2005 increase as the annual decline in limits grow in magnitude (i.e., tighter limits). For example, under N1 and N7 scenarios, $\text{NO}_3\text{-N}$ concentration declines 1.8% and 99%, respectively, over the eight years. Interestingly, detected under Base, N1, N2, and N3 scenarios, P concentration had a higher concentration in 2005 compared to 1998. This could be attributed to the fact that although cotton was associated with the second highest P load (behind Bermuda), associated $\text{NO}_3\text{-N}$ loadings were relatively low; thus, up until some point at least, it remains practical and profitable to continue agriculture producing cotton. For remaining scenarios up to N7, P concentration generally declined year over year, with N7 exhibiting the most significant decline in P concentration (11.1%). Meanwhile, P scenarios showed reduced

⁶ Aside from greater nutrient runoff, increased agricultural lands (depending on management practices) can also be the source of several other ecosystem disservices including loss of wildlife habitat and greenhouse gas emissions [63].

concentration in P and $\text{NO}_3\text{-N}$ derived over time. From 1998 to 2005, P concentration was reduced by 57.6% under P1 compared to a negative 68.6% under P7. Under these same scenarios, $\text{NO}_3\text{-N}$ concentration declined 16.5% and 23.1%, respectively. The combined NP scenarios follow a similar pattern where $\text{NO}_3\text{-N}$ and P concentration fell by 16.6% and 57.8% respectively in NP1 compared with NP7 for which $\text{NO}_3\text{-N}$ concentration reduced by 69.1% and P concentration decreased by 65.0%. Bosch et al. [65], in comparison, found no clear relationship among changes in land cover or management practices on nutrient loads. Cho et al. [17], in their analysis of NPS pollution impacts from different management practices, found the single greatest contributor to NPS pollutant reduction in the LREW was that of current riparian forest cover levels (riparian forest buffers offered the most comprehensive reduction in total phosphorous (19.5%) and total nitrogen (7.0%)).

5.1. Key study caveats

The fundamental goal driving our study design was to provide a conceptual overview of the core model framework and demonstrate its potential with a working application. Nonetheless, key caveats to our study follow. Constraints on the maximum number of hectares for each crop at a particular period may be called for since it is likely that in any given year, an entire sub-basin would (could) not convert to 100% of a certain crop. Of greater matter are environmental uncertainties regarding amounts of nutrient load or precipitation, which in turn would affect recorded surface runoff that may warrant inclusion in future applications; and, similarly, economic fluctuations captured through historical crop price volatility. Further, while we assume zero nutrient loadings and zero profits in an attempt keep land categorized as Extra (i.e., any land not considered part of our six major land use categories) neutral, we realize in the case of barren land, included as part of Extra, no erosion and consequently sediment and phosphorus loads are likely to occur. However, considering Extra constitutes almost a quarter (23%) of the total watershed area, the current study may suffer from a limitation in this regard.

From a policy perspective, water quality constraints, which mandate increasing stringency over a nine-year period could be regarded as too theoretical from a policy perspective. To add further complexity, one may argue substantial spatially distributed time lags exist between actions on the surface and the response in streams where numeric nutrient criteria must be met. One solution would be to introduce appropriate time lags provided a generous dataset. An alternative might involve exploiting large temporal datasets to develop optimal land use configurations for a single water quality constraint (over a decadal or more climate sequence) with year-to-year price uncertainty. Yet as the temporal (or spatial) scale increases, trade-offs inevitably become more ambiguous and challenging to quantify.

In terms of nutrient legacies, SWAT to some degree, can handle these effects, but it is not the ideal tool for it. Even if one were to shut down all the nutrient inputs, the nutrient concentrations would slowly decrease in SWAT simulations. SWAT considers multiple pools for N and P. Each pool undergoes reactions (e.g., transformation and decay). They are also transported between different systems in the watershed. It takes time for nitrate, for example, to move from the top of the soil to the groundwater. There it remains for a while but undergoes a decay process before it is released to streams. Our simulation period is nearly two decades. Longer periods are more desirable to better capture the legacy effects. Additionally, we acknowledge SWAT is not the perfect tool to capture legacy effects, and other tools should be evaluated for better exploring the watershed dynamics in the study area.

Due to such data limitations, our study timeframe is restricted to nine years; yet the above concerns remain valid. Model modifications will need to be made where deemed appropriate. This also opens avenues for future research. For example, an additional dimension such as a particular BMP could be extended to the framework (Fig. S5) to strategically target optimal land management regimes across the watershed. Contemporary BMPs in the LREW have been documented to include riparian forest buffers, contour farming, and cover crops for conservation tillage systems [17,32,65]. Undoubtedly, depending on the size of a particular dimension (e.g., number of sub-basins) as well as the number of dimensions themselves (e.g., incorporating additional features such as HRU or management style), the breadth of the problem can grow quite large.

Lastly, our new approach offers more indications to policymakers rather than landowners. The SWAT model as described here is based on sub-basins and HRUs (unique combinations of soil, land use and slope) and not set-up at the farm level, therefore, it is harder to, based on SWAT results, provide landowners guidelines to specific crops in their fields. It can, however, provide indications to policymakers on where certain measures can be more effective in reducing non-point sources nutrients runoff at the watershed outlet. Moreover, though the lens of policy uncertainties, it is unlikely for such a nutrient limit constraint (i.e., policy) to exist exactly as we have specified. But results from using the proposed model do provide generalized results of where and possibly when changes in land cover may have to be implemented to realize local water quality targets.

6. Conclusion

This study combined estimates for nutrient load and surface runoff from a calibrated and validated SWAT model with profits by crop type to construct a dynamic LP problem capable of gauging impacts on aggregate watershed profits due to conforming to nutrient concentration criteria at the watershed outlet. The model allows the researcher to identify dynamic patterns in land use evolution at the sub-basin level. Our study concludes with three important findings in light of obtained results. First, compliance with different nutrient load criteria may produce substantial relative differences in the impact on land cover. While the general pattern can be described as a shift towards forestland, results can vary drastically in terms of total acres converted and forest type. Second, compliance with prescribed limits on numeric nutrient criteria is expected to reduce aggregate landowner profit, but the degree of profit reduction will directly depend on land use decisions. The disparity in profits between the particular nutrient content measured (i.e., in our case, $\text{NO}_3\text{-N}$ or P) may be more pronounced depending on relative price differences among crops considered. Third, a close examination of

dual prices reveals sensitivity could vary greatly depending on how restrictive the water quality limits are. *Ceteris paribus*, our results showed greater sensitivity as permittable concentration amounts shrank and greater dual prices associated with NO₃-N constraints (to comparable P constraints).

It is essential to keep in mind this is a methods-based study and should be inferred as such. Although the LREW is devoid of apparent water quality issues, the watershed was selected in part since it served as a convenient source of comprehensive hydrological and nutrient data. Yet, due to its relative ease in scaling up (in terms of allowing for a greater number of spatial units, crops or time periods) as well as its capacity to take on a greater number of dimensions/extensions (e.g., perhaps incorporating crop-specific management regimes associated with each spatial unit per time step), we hope our model construct may serve as a general template to establish ideal cropping patterns under hypothetical ambient standards in water quality downstream for other watersheds.

Author statement

This study was conceptualized and designed by Dr. Ranjit Bawa and Dr. Puneet Dwivedi. Dr. Ranjit Bawa was responsible for data curation and analysis. Dr. Puneet Dwivedi provided guidance on the original draft preparation and editing. Dr. Nahal Hoghooghi and Dr. Latif Kalin provided instrumental feedback on the hydrological methodology, editing and review of the manuscript. Dr. Huang also provided editing and review of the manuscript.

Declaration of competing interest

The authors declare that they have no known competing financial interests or personal relationships that could have appeared to influence the work reported in this paper.

Data availability

The authors are unable or have chosen not to specify which data has been used.

Acknowledgement

This material is based upon work that is supported by the National Institute of Food and Agriculture, US Department of Agriculture, under award number 2017-68007-26319.

Appendix A. Supplementary data

Supplementary data to this article can be found online at <https://doi.org/10.1016/j.wre.2022.100209>.

References

- [1] R. Qadri, M.A. Faiq, Freshwater pollution: effects on aquatic life and human health, in: Fresh Water Pollution Dynamics and Remediation, Springer, Singapore, 2020, pp. 15–26.
- [2] L. Schweitzer, J. Noblet, Water contamination and pollution, in: Green Chemistry, Elsevier, 2018, pp. 261–290.
- [3] C.M. Villanueva, M. Kogevinas, S. Cordier, M.R. Templeton, R. Vermeulen, J.R. Nuckols, M. Nieuwenhuijsen, P. Levallois, Assessing exposure and health consequences of chemicals in drinking water: current state of knowledge and research needs, *Environ. Health Perspect.* 122 (3) (2014) 213–221.
- [4] S.R. Carpenter, Phosphorus control is critical to mitigating eutrophication, *Proc. Natl. Acad. Sci. USA* 105 (32) (2008) 11039–11040.
- [5] D. Brogna, A. Michez, S. Jacobs, M. Dufrêne, C. Vincke, N. Dendoncker, Linking forest cover to water quality: a multivariate analysis of large monitoring datasets, *Water* 9 (3) (2017) 176.
- [6] J. Fiquepron, S. Garcia, A. Stenger, Land use impact on water quality: valuing forest services in terms of the water supply sector, *J. Environ. Manag.* 126 (2013) 113–121.
- [7] D.G. Neary, G.G. Ice, C.R. Jackson, Linkages between forest soils and water quality and quantity, *For. Ecol. Manag.* 258 (10) (2009) 2269–2281.
- [8] J. Tu, Spatially varying relationships between land use and water quality across an urbanization gradient explored by geographically weighted regression, *Appl. Geogr.* 31 (1) (2011) 376–392.
- [9] J.D. Allan, Landscapes and riverscapes: the influence of land use on stream ecosystems, *Annu. Rev. Ecol. Evol. Syst.* 35 (2004) 257–284.
- [10] R. Bawa, P. Dwivedi, Impact of land cover on groundwater quality in the Upper Floridan Aquifer in Florida, United States, *Environ. Pollut.* 252 (2019) 1828–1840.
- [11] R.K. Hubbard, J.M. Sheridan, R. Lowrance, D.D. Bosch, G. Vellidis, Fate of nitrogen from agriculture in the southeastern Coastal Plain, *J. Soil Water Conserv.* 59 (2) (2004) 72–86.
- [12] R. Wan, S. Cai, H. Li, G. Yang, Z. Li, X. Nie, Inferring land use and land cover impact on stream water quality using a Bayesian hierarchical modeling approach in the Xitiaozi River Watershed, China, *J. Environ. Manag.* 133 (2014) 1–11.
- [13] U.S. Environmental Protection Agency (USEPA), Quality Criteria for Water 1986, U.S. Environmental Protection Agency, Washington, D.C., 1986, p. 453. Report 440/5-86-001.
- [14] Georgia Environmental Protection Division, Georgia's Plan for the Adoption of Water Quality Standards for Nutrients, Georgia Dept. of Natural Resources Environmental Protection Division, Atlanta, GA, 2013.
- [15] U.S. Environmental Protection Agency (USEPA), 40 CFR Part 131 "Water Quality Standards: Establishment of Numeric Criteria for Priority Toxic Pollutants for the State of California." 40 CFR Part 131, USEPA, Washington, D.C., 2000.
- [16] D.D. Bosch, J.M. Sheridan, H.L. Batten, J.G. Arnold, Evaluation of the SWAT model on a coastal plain agricultural watershed, *Transactions of the ASAE* 47 (5) (2004) 1493.

- [17] J. Cho, G. Vellidis, D.D. Bosch, R. Lowrance, T. Strickland, Water quality effects of simulated conservation practice scenarios in the Little River Experimental watershed, *J. Soil Water Conserv.* 65 (6) (2010) 463–473.
- [18] G.W. Feyerisen, T.C. Strickland, D.D. Bosch, D.G. Sullivan, Evaluation of SWAT manual calibration and input parameter sensitivity in the Little River watershed, *Trans. ASABE* 50 (3) (2007) 843–855.
- [19] M.W. Van Liew, J.G. Arnold, D.D. Bosch, Problems and potential of autocalibrating a hydrologic model, *Transactions of the ASAE* 48 (3) (2005) 1025–1040.
- [20] E.J.B. Gaddis, A. Voinov, R. Seppelt, D.M. Rizzo, Spatial optimization of best management practices to attain water quality targets, *Water Resour. Manag.* 28 (6) (2014) 1485–1499.
- [21] P. Srivastava, J.M. Hamlett, P.D. Robillard, R.L. Day, Watershed optimization of best management practices using AnnAGNPS and a genetic algorithm, *Water Resour. Res.* 38 (3) (2002) 3, 1.
- [22] T.L. Veith, M.L. Wolfe, C.D. Heatwole, Optimization procedure for cost effective bmp placement at a watershed scale 1, *JAWRA J. Am. Water Resour. Assoc.* 39 (6) (2003) 1331–1343.
- [23] L. Shoemaker, J. Riverson, K. Alvi, J.X. Zhen, S. Paul, T. Rafi, A Framework for Placement of Best Management Practices in Urban Watersheds to Protect Water Quality, United States Environmental Protection Agency. National Risk Management Research Laboratory Office of Research and Development U.S. Environmental Protection Agency, 2009.
- [24] J.F. Limbrunner, R.M. Vogel, S.C. Chapra, P.H. Kirshen, Classic optimization techniques applied to stormwater and nonpoint source pollution management at the watershed scale, *J. Water Resour. Plann. Manag.* 139 (5) (2013) 486–491.
- [25] B.K. Pokhrel, K.P. Paudel, Assessing the efficiency of alternative best management practices to reduce nonpoint source pollution in a rural watershed located in Louisiana, USA, *Water* 11 (8) (2019) 1714.
- [26] A. Sebti, M. Fuamba, S. Bennis, Optimization model for BMP selection and placement in a combined sewer, *J. Water Resour. Plann. Manag.* 142 (3) (2015), 04015068.
- [27] D.H. Burn, E.A. McBean, Optimization modeling of water quality in an uncertain environment, *Water Resour. Res.* 21 (7) (1985) 934–940.
- [28] Y. Jia, T.B. Culver, Robust optimization for total maximum daily load allocations, *Water Resour. Res.* 42 (2) (2006).
- [29] P.V. Femeena, K.P. Sudheer, R. Cibin, I. Chaubey, Spatial optimization of cropping pattern for sustainable food and biofuel production with minimal downstream pollution, *J. Environ. Manag.* 212 (2018) 198–209.
- [30] Y. Zhou, B. Yang, J. Han, Y. Huang, Robust linear programming and its application to water and environmental decision-making under uncertainty, *Sustainability* 11 (1) (2019) 33.
- [31] A. Kaim, M. Strauch, M. Volk, Using stakeholder preferences to identify optimal land use configurations, *Front. Water* 2 (2020) 63.
- [32] D.G. Sullivan, H.L. Batten, D. Bosch, J. Sheridan, T. Strickland, Little river experimental watershed, Tifton, Georgia, United States: a geographic database, *Water Resour. Res.* 43 (9) (2007).
- [33] D.D. Bosch, J.M. Sheridan, F.M. Davis, Rainfall characteristics and spatial correlation for the Georgia Coastal Plain, *Transactions of the ASAE* 42 (6) (1999) 1637.
- [34] Conservation Effects Assessment Project, Conservation effects assessment project – the ARS watershed assessment study, Available at: https://www.nrcs.usda.gov/Internet/FSE_DOCUMENTS/nrcs143_012923.pdf, 2005.
- [35] J.G. Arnold, D.N. Moriasi, P.W. Gassman, K.C. Abbaspoor, M.J. White, R. Srinivasan, N. Kannan, SWAT: model use, calibration, and validation, *Trans. ASABE* 55 (4) (2012) 1491–1508.
- [36] P.W. Gassman, M.R. Reyes, C.H. Green, J.G. Arnold, The soil and water assessment tool: historical development, applications, and future research directions, *Trans. ASABE* 50 (4) (2007) 1211–1250.
- [37] S. Shrestha, P. Dwivedi, S.K. McKay, D. Radcliffe, Assessing the potential impact of rising production of industrial wood pellets on streamflow in the presence of projected changes in land use and climate: a case study from the oconee River Basin in Georgia, United States, *Water* 11 (1) (2019) 142.
- [38] G.L. Hargreaves, G.H. Hargreaves, J.P. Riley, Agricultural benefits for Senegal River basin, *J. Irrigat. Drain. Eng.* 111 (2) (1985) 113–124.
- [39] J.G. Arnold, N. Fohrer, SWAT2000: current capabilities and research opportunities in applied watershed modelling, *Hydrol. Process.: Int. J.* 19 (3) (2005) 563–572.
- [40] J.G. Arnold, P.M. Allen, R. Muttiah, G. Bernhardt, Automated base flow separation and recession analysis techniques, *Groundwater* 33 (6) (1995) 1010–1019.
- [41] K.C. Abbaspoor, E. Rouholahnejad, S. Vaghefi, R. Srinivasan, H. Yang, B. Kløve, A continental-scale hydrology and water quality model for Europe: calibration and uncertainty of a high-resolution large-scale SWAT model, *J. Hydrol.* 524 (2015) 733–752.
- [42] K.C. Abbaspoor, J. Yang, I. Maximov, R. Siber, K. Bogner, J. Mieleitner, R. Srinivasan, Modelling hydrology and water quality in the pre-alpine/alpine Thur watershed using SWAT, *J. Hydrol.* 333 (2–4) (2007) 413–430.
- [43] H.V. Gupta, H. Kling, K.K. Yilmaz, G.F. Martinez, Decomposition of the mean squared error and NSE performance criteria: implications for improving hydrological modelling, *J. Hydrol.* 377 (1–2) (2009) 80–91.
- [44] J.E. Nash, J.V. Sutcliffe, River flow forecasting through conceptual models part I—a discussion of principles, *J. Hydrol.* 10 (3) (1970) 282–290.
- [45] D.N. Moriasi, J.G. Arnold, M.W. Van Liew, R.L. Bingner, R.D. Harmel, T.L. Veith, Model evaluation guidelines for systematic quantification of accuracy in watershed simulations, *Trans. ASABE* 50 (3) (2007) 885–900.
- [46] D.N. Moriasi, M.W. Gitau, N. Pai, P. Daggupati, Hydrologic and water quality models: performance measures and evaluation criteria, *Trans. ASABE* 58 (6) (2015) 1763–1785.
- [47] D.N. Moriasi, B.N. Wilson, K.R. Douglas-Mankin, J.G. Arnold, P.H. Gowda, Hydrologic and water quality models: use, calibration, and validation, *Trans. ASABE* 55 (4) (2012) 1241–1247.
- [48] L. Kalin, M.M. Hantush, An auxiliary method to reduce potential adverse impacts of projected land developments: subwatershed prioritization, *Environ. Manag.* 43 (2) (2009) 311.
- [49] N. Noori, L. Kalin, S. Sen, P. Srivastava, C. Lebleu, Identifying areas sensitive to land use/land cover change for downstream flooding in a coastal Alabama watershed, *Reg. Environ. Change* 16 (6) (2016) 1833–1845.
- [50] B. Saghafian, M. Khosroshahi, Unit response approach for priority determination of flood source areas, *J. Hydrol. Eng.* 10 (4) (2005) 270–277.
- [51] C. Schürz, SWATplusR: Running SWAT2012 and SWAT+ Projects in R, 2019, <https://doi.org/10.5281/zenodo.3373859>. R package version 0.2.7, <https://github.com/chrischuerz/SWATplusR>.
- [52] USDA National Agricultural Statistics Service, Available at: <https://data.nal.usda.gov/dataset/nass-quick-stats>, 2019.
- [53] TimberMart-South (TMS), TimberMart-South Quarterly Report, Norris foundation, Daniel B. Warnell School of Forest Resources. University of Georgia, Athens, GA, 2019.
- [54] University of Georgia, College of Agricultural & Environmental Sciences, Extension, Historical crop budgets, Available at: <https://agecon.uga.edu/extension/budgets/historical-budgets.html>, 2020.
- [55] A. Maggard, R. Barlow, Costs and trends for Southern forestry practices [Special Report], *For. Landowner* 76 (5) (2016) 31–39.
- [56] Lindo Systems, What'sBest! the Spreadsheet Solver, , Lindo Systems Inc, 2019. <http://www.lindo.com>.
- [57] L.J. Zhu, C.Z. Qin, A. Zhu, J. Liu, H. Wu, Effects of different spatial configuration units for the spatial optimization of watershed best management practice scenarios, *Water* 11 (2) (2019) 262.
- [58] R.K. Hubbard, Characteristics of Selected Upland Soils of the Georgia Coastal Plain, ARS, USA, 1985.
- [59] E. Nelson, G. Mendoza, J. Regetz, S. Polasky, H. Tallis, D. Cameron, K.M. Chan, G.C. Daily, J. Goldstein, P.M. Kareiva, E. Lonsdorf, R. Naidoo, T.H. Ricketts, M. Shaw, Modeling multiple ecosystem services, biodiversity conservation, commodity production, and tradeoffs at landscape scales, *Front. Ecol. Environ.* 7 (1) (2009) 4–11.
- [60] A. Weersink, J. Livernois, J.F. Shogren, J.S. Shortle, Economic Instruments and Environmental Policy in Agriculture, Canadian Public Policy/Analyse de Politiques, 1998, pp. 309–327.
- [61] A.G. Power, Ecosystem services and agriculture: tradeoffs and synergies, *Phil. Trans. Biol. Sci.* 365 (1554) (2010) 2959–2971.

- [64] S. Pfister, P. Bayer, A. Koehler, S. Hellweg, Environmental impacts of water use in global crop production: hotspots and trade-offs with land use, *Environ. Sci. Technol.* 45 (13) (2011) 5761–5768.
- [65] D.D. Bosch, O. Pisani, A.W. Coffin, T.C. Strickland, Water quality and land cover in the Coastal Plain Little River watershed, Georgia, United States, *J. Soil Water Conserv.* 75 (3) (2020) 263–277.
- [66] G.W. Feyereisen, R. Lowrance, T.C. Strickland, D.D. Bosch, J.M. Sheridan, Long-term stream chemistry trends in the southern Georgia Little River Experimental watershed, *J. Soil Water Conserv.* 63 (6) (2008) 475–486.
- [67] M.I. Trodahl, B.M. Jackson, J.R. Deslippe, A.K. Metherell, Investigating trade-offs between water quality and agricultural productivity using the Land Utilisation and Capability Indicator (LUCI)-a New Zealand application, *Ecosyst. Serv.* 26 (2017) 388–399.
- [70] Environmental Protection Agency, Ecoregion nutrient criteria documents for rivers and streams, 2002. Available online at www.epa.gov/waterscience/criteria/nutrient/ecoregions/rivers/.